Simulations of the axisymmetric magnetospheres of neutron stars

S. S. Komissarov★

Department of Applied Mathematics, The University of Leeds, Leeds LS2 9GT

ABSTRACT

In this paper we present the results of time-dependent simulations of the dipolar axisymmetric magnetospheres of neutron stars carried out within the frameworks of both relativistic magnetohydrodynamics (MHD) and resistive force-free electrodynamics. The results of force-free simulations reveal the inability of our numerical method to accommodate the equatorial current sheets of pulsar magnetospheres, and raise a question mark about the robustness of this approach. On the other hand, the MHD approach allows us to make significant progress. We start with a non-rotating magnetically dominated dipolar magnetosphere and follow its evolution as the stellar rotation is switched on. We find that the time-dependent solution gradually approaches a steady state that is very close to the stationary solution of the pulsar equation found in 1999 by Contopoulos, Kazanas & Fendt. This result suggests that other stationary solutions that have the Y-point located well inside the light cylinder are unstable. The role of particle inertia and pressure on the structure and dynamics of MHD magnetospheres is studied in detail, as well as the potential implications of dissipative processes in the equatorial current sheet. We argue that pulsars may have differentially rotating magnetospheres which develop noticeable structural oscillations, and that this may help to explain the nature of the subpulse phenomena.

Key words: MHD – relativity – pulsars: general – stars: winds and outflows.

1 INTRODUCTION

Pulsar magnetospheres are complicated electrodynamic systems that involve the acceleration of charged particles by the rotationally induced electric field, electron–positron pair production, and the bulk outflow of magnetospheric plasma through the light cylinder. Pair production presumably occurs on a scale that is significantly smaller than the magnetospheric scale (the latter is determined by the light cylinder radius $\varpi_{\rm lc} = c/\Omega$). This suggests that the global structure of pulsar magnetospheres may not depend on the details of the pair production mechanism, which may enter the problem only in the form of boundary conditions. The simplest assumption is that the plasma supply is sufficiently plentiful to allow the magnetohydrodynamic (MHD) description throughout the whole magnetosphere. Although this may not be so in the case of slowly rotating or weakly magnetized pulsars (Hibschman & Arons 2001), it still makes sense to regard the MHD solution as a zero approximation model and a good reference point.

Although pulsar magnetospheres are generically three-dimensional, it is still reasonable to start with a much simpler axisymmetric case, as it involves most of the basic physical elements of the general case. Michel (1973) and Scharlemann

& Wagoner (1973) first analysed the structure of a stationary axisymmetric pulsar magnetosphere in the limit of force-free electrodynamics where both the pressure and the inertia of the magnetospheric plasma are assumed to be vanishingly small. They found that in this case the problem reduces to the following second-order partial differential equation (PDE), which is now called the pulsar equation:

$$(1 - x^2)\left(\frac{\partial^2 \Psi}{\partial x^2} + \frac{1}{x}\frac{\partial \Psi}{\partial x} + \frac{\partial^2 \Psi}{\partial y^2}\right) - \frac{2}{x}\frac{\partial \Psi}{\partial x} = -\mathcal{A}(\Psi)\frac{\mathrm{d}\mathcal{A}}{\mathrm{d}\Psi}. \quad (1)$$

Here $x = \varpi/\varpi_{\rm lc}$ and $y = z/\varpi_{\rm lc}$ are the cylindrical coordinates normalized to the radius of the light cylinder and Ψ is the magnetic flux function. This equation also involves the poloidal current function, $\mathcal{A}(\Psi)$, which is unknown. If this function is somehow specified, the pulsar equation becomes a linear elliptic equation. However, the question of what actually determines the electric current function is not that obvious and is still debated (Mestel 1999; Beskin 2005). The physical meaning of these functions is quite simple: $\Psi = \Phi/2\pi$, where $\Phi(x, y)$ is the magnetic flux through the axisymmetric circular loop given by $x = $ constant, $y = $ constant; and $\mathcal{A} = 2I/c$, where $I(x, y)$ is the total electric current flowing through the same loop. It is also worth mentioning that, if we set $A_\phi(x = 0) = 0$, then $\Psi = A_\phi$, and that, in a steady state, $\mathcal{A} = H_\phi$, where A_ϕ and H_ϕ are the covariant azimuthal components of the vector potential $\boldsymbol{A}$ and the magnetic field $\boldsymbol{H}$ in the non-normalized basis of cylindrical or spherical coordinates.

★E-mail: serguei@maths.leeds.ac.uk

Another important feature of this equation is the mathematical singularity at the light cylinder. It was argued by Ingraham (1973) that the condition of smooth passage through this surface together with the appropriate boundary conditions determine the unique electric current function of the pulsar equation. (This property makes the problem somewhat similar to the classical eigenvalue problem in the theory of differential equations.) Ingraham (1973) even proposed an iterative algorithm for finding this function. In the same year Michel (1973) did actually find an exact solution to the pulsar equation in the case of a split-monopole magnetic field that passed through the singular surface both continuously and smoothly. Although Michel did not use Ingraham's approach, his result supported Ingraham's idea and raised expectations for finding smooth continuous solutions in more complicated realistic cases, like for example the magnetosphere of a rotating dipole, as well. [The recent observations of magnetospheric eclipses in the binary pulsar J0737−3039 have confirmed that the dipolar model may indeed be quite accurate (Lyutikov & Thompson 2005).]

The electric current of Michel's (1973) solution has the same sign within the magnetosphere, with the exception of the equatorial current sheet that provides current closure. Further analysis by Ingraham (1973) and Michel (1974) suggested that, if the force-free solution for an axisymmetric rotating dipole existed, then far beyond the light cylinder it should still closely resemble the split-monopole one. However, in the near zone the structure of the dipolar magnetosphere was expected to be qualitatively different. Indeed, close to the star the effects of its rotation are relatively small and so must be the difference between the solutions for the rotating and the non-rotating magnetospheres. As a result, a so-called 'dead zone' should exist where the magnetic field lines remain closed and the magnetospheric plasma corotates with the star.

However, the problem of finding the self-consistent global solution for dipolar magnetospheres turned out to be rather involved, even for the axisymmetric case of aligned rotator. For a very long time, the only attempts to construct such solutions involved the utilization of prescribed electric current functions. Such solutions would either exhibit kinks at the light cylinder or violate the conditions of the force-free approximation at some relatively short distance from it (e.g. Michel 1982; Beskin, Gurevich & Istomin 1993). The breakthrough came only recently when Contopoulos, Kazanas & Fendt (1999, hereafter CKF) finally managed to solve the problem numerically. In this solution, the dead zone continues all the way to the light cylinder where the so-called 'Y-point' appears in the magnetic field structure, whereas beyond the light cylinder it has the same topology as the split-monopole solution including an infinitely thin equatorial current sheet. The return current of the equatorial current sheet splits at the Y-point into two current sheets that flow along the surface separating the dead zone from the open field zone. An additional finite-width layer of return current exists just outside of the dead zone and around the equatorial plane.

Uzdensky (2003) carried out an asymptotic analysis of the force-free solutions in the vicinity of the Y-point. It turned out that in the presence of separating current sheets, similar to those found in Contopoulos et al. (1999), the electromagnetic field becomes infinitely strong at the Y-point. Uzdensky (2003) argued that this is unphysical and questioned the correctness of the CKF solution. As an alternative he considered the case with no current sheets, i.e. the case where the electric current returns within the equatorial layer of the open field zone only. In this case the electromagnetic field does not diverge at the Y-point, but just outside of this point the electric field becomes stronger than the magnetic field, signalling a breakdown of the force-free approximation. No such complications

were found for the Y-point located inside the light cylinder. In fact, in this case the separating surface crosses the equator at the right angle so that the Y-point turns into a 'T-point'.

Gruzinov (2005) also analysed the force-free solution in the vicinity of the Y-point located at the light cylinder in the presence of current sheets and confirmed that in this case the electromagnetic field diverges at the Y-point. His analytical solution exhibits an angle of 77.3 degrees between the equatorial plane and the separating surface at the Y-point. In order to verify this, Gruzinov (2005) repeated the calculations of CKF with much higher spatial resolution, and the results seemed to confirm the development of a singularity with the expected inclination angle of separatrices.

The next potentially very important step was made by Goodwin et al. (2004), who realized that the dead zone does not have to extend all the way to the light cylinder but can be much smaller. Such solutions select their own electric current functions, smaller dead zones corresponding to weaker currents. In fact, the first solutions of the pulsar equation, which described both the equatorial current sheet and the dead zones that were located deep inside the light cylinder, were found by Lyubarskii (1990). However, these solutions utilized a prescribed electric current function and, as a result, exhibited the breakdown of the force-free approximation – at a certain distance from the light cylinder the electric field became stronger than the magnetic field. Goodwin et al. (2004) also included finite gas pressure inside the dead zone and showed that this allows solutions that remain non-singular at the Y-point even when this point is located on the light cylinder. In this case their solution gives an inclination angle of the Y-point of 56.5 degrees. However, the inertia associated with the gas pressure has not been taken into account, and thus the self-consistency of such an approach is questionable. This idea of Goodwin et al. (2004) was further explored by Timokhin (2005), who constructed numerical solutions for force-free magnetospheres with the Y-point located within the light cylinder (with no finite gas pressure in the dead zone). He also pointed out that the pulsar spin-down rate depended not only on the size the light cylinder but also on the size of the dead zone, and if the ratio of these scales were to evolve with the pulsar age then this could explain why the observed braking index of pulsars is smaller than the value derived from the models with the dead zone extending all the way up to the light cylinder.

Another interesting twist has been added by Contopoulos (2005), who argued that during pulsar evolution the potential gap separating the star surface from the polar-cap magnetosphere grows in magnitude leading to a slower rotation of the open field lines compared to the star and the dead zone. In such a case, there is no a single light cylinder for the whole magnetosphere. Instead, the dead zone has its own light cylinder that is located inside the light cylinder of the polar cap. To illustrate this point, Contopoulos (2005) constructed a set of numerical models of pulsar magnetospheres of this kind. The evolution of the angular velocity of the polar-cap magnetosphere with pulsar age may also result in lower values of the pulsar's braking index.

In spite of this remarkable progress, the method of pulsar equation has its obvious limitations. It does not address the question of the stability of the steady-state solutions, and it does not allow us to study possible non-stationary phenomena in pulsar magnetospheres. Moreover, the numerical techniques that have been used to solve the pulsar equation may turn out to be rather difficult to adapt to the fully three-dimensional problem of the oblique rotator. The obvious way of approaching these problems is to relax the stationarity condition and to solve the original system of time-dependent equations. Although force-free electrodynamics has been used to

model various astrophysical systems since the 1970s, the focus was entirely on the steady-state equations. Only recently have the time-dependent equations been subjected to a systematic study (Uchida 1997; Gruzinov 1999; Punsly 2003; Komissarov 2002a). As a result it has been found that they form a simple hyperbolic system of conservation laws in many respects similar to relativistic MHD but only with the fast and the Alfvén hyperbolic waves (Komissarov 2002a). Thus, a variety of standard numerical methods can be used to deal with these equations. The very first numerical simulations of this kind, of the monopolar magnetospheres of black holes, seemed to confirm the suitability of this approach (Komissarov 2001). However, further applications to somewhat more complex magnetic configurations revealed its limitations, as the force-free approximation would often break down following the development of strong current sheets (Komissarov 2002a,b; Spitkovsky 2004; Asano, Uchida & Matsumoto 2005). These results suggested the need to look for a more general mathematical framework that would allow current sheets to be handled via the introduction of new channels of back-reaction of plasma on the electromagnetic field. One of the most suitable options is the framework of resistive relativistic MHD. However, this approach remains rather poorly studied even now. Ideal relativistic MHD is a somewhat easier option and, thanks to recent efforts by several groups, significant expertise has been obtained in developing numerical methods for this system. This approach allows us to take into account the thermodynamic pressure of plasma heated in the current sheets, but the dissipation of electromagnetic energy is entirely due to numerical resistivity, which is not fully satisfactory.

Another alternative is resistive force-free electrodynamics with physical or artificial resistivity. If the current sheets of pulsar magnetospheres are indeed dissipationless, then this approach might work provided that the utilized Ohm's law allows evolution towards a dissipationless force-free state. The recent time-dependent simulations by Spitkovsky show that this approach may indeed be quite productive (the results were presented in the summer of 2005 at the conference on the 'Physics of Astrophysical Outflows and Accretion Discs', Kavli Institute for Theoretical Physics, Santa Barbara, CA.)

In this paper we report the results of new time-dependent axisymmetric simulations of rotating dipolar magnetospheres of neutron stars within the frameworks of resistive force-free electrodynamics and ideal relativistic MHD. We only consider the case where the whole magnetosphere rotates with the same angular velocity, and thus our results are not relevant to the model of Contopoulos (2005). This model will be the subject of a separate study. Note that throughout the paper the graphic data are shown in dimensionless units where the magnetic dipole moment $\mu = 1$, the angular velocity of the star Ω and the speed of light $c = 1$. Hence the cylindrical radius of the light cylinder $\varpi_{lc} = 1$.

2 COMMON FEATURES OF THE SIMULATIONS

Using the standard notation of the 3+1 approach, the metric form of a general space–time can be written as

$$ds^2 = (\beta^2 - \alpha^2)\,dt^2 + 2\beta_i\,dx^i\,dt + \gamma_{ij}\,dx^i\,dx^j, \tag{2}$$

where γ_{ij} is the metric tensor of 'the absolute space', α is the lapse function, and $\boldsymbol{\beta}$ is the shift vector. For most purposes in the physics of pulsar magnetospheres the flat space approximation suffices and one can enjoy the benefits of a global inertial frame where $\alpha = c$ and $\beta_i = 0$ (see however Beskin 1990; Muslimov & Tsygan 1990).

This is exactly what was adopted in the numerical models of pulsar magnetospheres described in the Introduction and in this study as well. However, the computer codes used in the simulations are designed to work with rather general axisymmetric and stationary space–times. Moreover, in the case of an oblique rotator, the frame rotating with the star seems to be more suitable as the solution may become stationary in this frame. In such a case $\boldsymbol{\beta}$ is no longer vanishing and in the basis of spherical spatial coordinates

$$\beta_r = \beta_\theta = 0, \qquad \beta_\phi = c\Omega \sin^2\theta\,r^2$$

and hence

$$\alpha^2 = c^2 \quad \text{and} \quad \beta^2 = c^2\Omega^2 \sin^2\theta\,r^2,$$

where Ω is the angular velocity of the frame.

In our simulations, the computational grid covers the axisymmetric domain $(r, \theta) = [r_{in}, r_{out}] \times [0, \pi]$, so no symmetry condition is enforced at the equatorial plane. The cell size in the r-direction is such that the corresponding physical lengths in both directions are equal, $\Delta r = r\,\Delta\theta$. The 'radiative' outer boundary, $r = r_{out}$, is always located so far away from the star that the light signal does not cross the computational domain by the end of the simulations – this ensures that waves produced near the star do not get reflected off the outer boundary at any rate.

As the Courant stability condition requires $\Delta t < \Delta r/c$, the suitable time-step for the outer part of the computational domain is much larger than that for its inner part. This allows us to reduce the computational cost of simulations via splitting the computational domain into a set of rings such that the outer radius of each ring is twice its inner radius and to advance the solution for each kth ring with its own time-step, Δt_k, such that $\Delta t_{k+1} = 2\Delta t_k$. Thus, one integration step of ring k corresponds to two integration steps of ring $k - 1$, four integration steps of ring $k - 2$ and so on. As a result, the outer regions of the computational domain are progressively less expensive in terms of CPU time. This approach has already been successfully applied in recent MHD simulations of pulsar wind nebulae (Komissarov & Lyubarsky 2004).

The initial solution describes a non-rotating magnetosphere with exactly dipolar magnetic field,

$$B^{\hat{\phi}} = 0,$$
$$B^{\hat{r}} = 2\mu \cos\theta/r^3, \tag{3}$$
$$B^{\hat{\theta}} = \mu \sin\theta/r^3,$$

where μ is the magnetic dipole moment. At time $t = 0$ the stellar rotation is suddenly switched on via an appropriate inner boundary condition. The simulations then proceed till it becomes clear whether or not the time-dependent solution relaxes to a steady state on scales comparable with the light cylinder radius. Steady-state solutions that are found in such a way are automatically stable to axisymmetric perturbations with wavelengths exceeding the cell size.

3 ELECTRODYNAMIC MODEL

3.1 Equations

Following Komissarov (2004a) we write the vacuum Maxwell's equations as

$$\partial_i(\sqrt{\gamma}\,B^i) = 0, \tag{4}$$

$$(1/c)\,\partial_t B^i + e^{ijk}\,\partial_j E_k = 0, \tag{5}$$

$$\partial_i(\sqrt{\gamma}\,D^i) = 4\pi\sqrt{\gamma}\,\kappa, \tag{6}$$

$$-(1/c)\,\partial_t D^i + e^{ijk}\,\partial_j H_k = (4\pi/c)J^i. \tag{7}$$

Here $\gamma = \det(\gamma_{ij})$ is the determinant of the metric tensor of the absolute space, and $e_{ijk} = \sqrt{\gamma}\,\epsilon_{ijk}$ is the Levi–Civita tensor of the absolute space ($\epsilon_{123} = 1$ for right-handed systems and $\epsilon_{123} = -1$ for left-handed ones). The electric field, $\boldsymbol{E}$, and the magnetic field, $\boldsymbol{B}$, are defined via

$$E_i = \tfrac{1}{2}\alpha e_{ijk}\,^*F^{jk} \tag{8}$$

and

$$B^i = \alpha\,^*F^{it}. \tag{9}$$

Here $^*F^{\mu\nu}$ is the Faraday tensor of the electromagnetic field, which is simply dual to the Maxwell tensor $F^{\mu\nu}$:

$$^*F^{\alpha\beta} = \tfrac{1}{2}e^{\alpha\beta\mu\nu}F_{\mu\nu}, \tag{10}$$

where

$$e_{\alpha\beta\mu\nu} = \sqrt{-g}\,\epsilon_{\alpha\beta\mu\nu} \tag{11}$$

is the Levi–Civita alternating tensor of space–time.

The differential equations (4)–(7) are supplemented with the following constitutive equations (Komissarov 2004a):

$$cE_k = \alpha D_k + e_{kij}\beta^i B^j, \tag{12}$$

$$cH_k = \alpha B_k - e_{kij}\beta^i D^j, \tag{13}$$

$$J^k = (\alpha/c)j^k - \kappa\beta^k. \tag{14}$$

Note that (1) the components of all the vectors and tensors appearing in these equations are measured in the non-normalized coordinate basis, $\{\partial_i\}$, of spatial coordinates; (2) $\boldsymbol{D}, \boldsymbol{B}, \boldsymbol{j}$ and κ are the electric field, magnetic field, electric current density and electric charge density as measured by a local observer at rest in the absolute space. The four velocity of this observer is

$$n^\nu = \frac{1}{\alpha}(c, \beta^i).$$

In the inertial frames of flat space–time, $\boldsymbol{E} = \boldsymbol{D}$ and $\boldsymbol{B} = \boldsymbol{H}$.

The final equation that is needed to close the system is Ohm's law. In strongly magnetized plasma the conductivity is no longer isotropic and under rather general conditions

$$\boldsymbol{j} = \sigma_\parallel \boldsymbol{D}_\parallel + \sigma_\perp \boldsymbol{D}_\perp + \boldsymbol{j}_d, \tag{15}$$

where

$$\boldsymbol{j}_d = \kappa c\,\frac{\boldsymbol{D} \times \boldsymbol{B}}{B^2} \tag{16}$$

is the drift current. Unless the magnetosphere has a scarce supply of electrically charged particles, i.e. is 'charge starved', the parallel conductivity is very large, which leads to a small residual parallel component of the electric field,

$$\sigma_\parallel \to \infty, \qquad \boldsymbol{D}_\parallel \to 0. \tag{17}$$

However, the strong magnetic field of pulsar magnetospheres effectively suppresses conductivity across the magnetic field lines (unless the electric field is even stronger than the magnetic one; this may be the case inside some current sheets). So we can put

$$\sigma_\perp = 0 \quad \text{if } B^2 > D^2. \tag{18}$$

As shown in Komissarov (2004a), in this limit we approach the approximation of force-free electrodynamics.

Within current sheets this simple prescription is unlikely to hold. On the one hand, in the area of high current density one may expect strong anomalous resistivity leading to significantly reduced $\sigma_\parallel$. As a result, the current sheet may become unstable to the tearing mode of reconnection (Lyutikov 2003). Since our intention at this point is merely to see if we can construct idealized numerical solutions that are more or less force-free and thus can be compared with the steady-state solutions of the pulsar equation, we will ignore this physical effect for the time being. On the other hand, the mere symmetry of the aligned rotator magnetosphere suggests that sooner or later the magnetic field of the force-free solution will become very small in the equatorial plane beyond the light cylinder, thus leading to unavoidable breakdown of the $D^2 < B^2$ condition of the force-free approximation. In such a case of relatively weak magnetic field the conductivity is expected to become much less anisotropic and we will assume that

$$\sigma_\perp = \sigma_\parallel \gg 1 \quad \text{if } B^2 < D^2. \tag{19}$$

Notice that the expression (16) for the drift current should also be modified in this case, as it implies that the drift speed

$$\boldsymbol{v}_d = c\,\frac{\boldsymbol{D} \times \boldsymbol{B}}{B^2} \tag{20}$$

becomes higher than the speed of light. We have tried several modifications for v_d, including

$$v_d = c\,\frac{\boldsymbol{D} \times \boldsymbol{B}}{\max(B^2, D^2)}, \tag{21}$$

which is likely to underestimate v_d in the current sheet, and

$$v_d = c\,\frac{\boldsymbol{D} \times \boldsymbol{B}}{|\boldsymbol{D} \times \boldsymbol{B}|} \quad \text{if } B^2 < D^2, \tag{22}$$
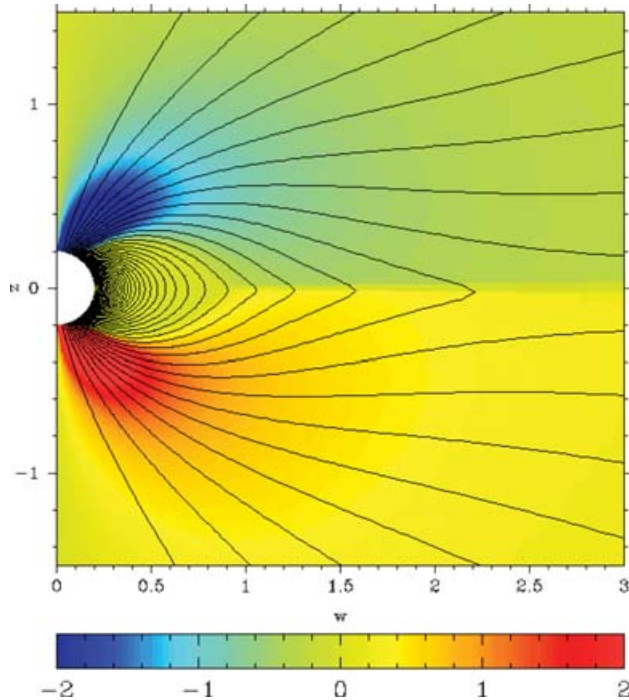
which certainly overestimates it. The actual value of the conductivity in the current sheet remains a free parameter.

To find numerical solutions of Maxwell's equation, in particular the solutions that are presented in the next section, we used the Godunov-type numerical scheme described in Komissarov (2004a).

3.2 Numerical simulations

The most striking and at first somewhat perplexing result of our electrodynamic simulations of pulsar magnetospheres is demonstrated in Fig. 1 – contrary to what is found in the steady-state solutions of the pulsar equation, the magnetic field lines remain close even outside of the light cylinder. Moreover, the solution seems to be rather insensitive to the details of the model for $\sigma_\perp$ and remains qualitatively the same even in the case $\sigma_\perp = 0$ (in fact, the solutions exhibited convergence in the limit $\sigma_\perp \to 0$).

The question of whether the field lines extending beyond the light cylinder should open up or not is in fact rather involved. One of the arguments often put forward in its discussion concerns the requirement for the speed of charged particles that fill the magnetosphere to remain smaller than the speed of light. In the drift approximation the charged particles move along the rotating magnetic field lines like beads on a wire – their motion is a composition of the rotational motion of the field line (the 'wire') and the sliding motion of the particle (the 'bead') along the field line. Within the light cylinder the speed of the rotational motion is less than the speed of light and the bead does not have to slide along the wire, but this is no longer the case beyond the light cylinder. Here the total speed of the bead can remain less than c only if it also slides along the wire and only if the wire is twisted in the azimuthal direction. (In such a case the sliding motion may help to reduce the azimuthal component of the bead velocity.) These conditions may well be satisfied everywhere along the open field lines but not along the closed ones. Indeed,

we find the following solution:

$$B^y = \begin{cases} -B & \text{if} \quad x < -1/\sigma_0, \\ B\sigma_0 x & \text{if} \quad -1/\sigma_0 < x < 1/\sigma_0, \\ B & \text{if} \quad x > 1/\sigma_0, \end{cases}$$

$$E^z = B.$$

This solution exhibits a number of interesting features. First of all it is stationary. Secondly, the magnitude of σ_0 effects only the width of the current sheet. This may explain the observed convergence of the magnetospheric solutions in the limit $\sigma_\perp \to 0$. Finally, the electromagnetic energy flows into the current sheet with the speed of light and disappears inside of it. This property clearly exposes the nature of Ohm's law (15) with prescription (23) or similar and outlines the limitations of its applicability. Indeed, in a real plasma Ohmic dissipation would cause strong heating and increase the gas pressure in the current sheet. This pressure would slow down the inflow of plasma into the current sheet and significantly modify its structure. However, this factor, as well as the plasma inertia, are completely ignored in our version of Ohm's law.

The fact that our numerical magnetospheric solution remains qualitatively the same even in the limit $\sigma_\perp = 0$ suggests that the numerical resistivity of our scheme takes over in this limit. Different numerical schemes have different dissipative properties and this may explain why the recent electrodynamic simulations of Spitkovsky (which have been presented at various astrophysical meetings) exhibit opening up of the field lines beyond the light cylinder and development of the dissipationless equatorial current sheet.

The properties of the current sheets of real pulsars are determined by a number of competing micro-physical processes that might be rather difficult to account for in a macroscopic model. Our experiments with the simplistic generalized Ohm's law (15)–(22) show that it facilitates the development of strongly dissipative current sheets. Since the dissipated energy of the electromagnetic field is not stored in any dynamical component and simply vanishes from the system, this model could only be relevant for magnetospheres with effective radiative cooling. The strong γ-ray emission from some pulsars may be interpreted as an indication of strong radiative current sheets (see the Discussion). Unfortunately, such emission is not a common feature of pulsars.

4 MHD MODEL

The difficulties that we have encountered in dealing with current sheets in force-free electrodynamics have forced us to return to the framework of full relativistic MHD even if the pulsar magnetospheres are expected to be magnetically dominated everywhere else and in spite of the fact that the system of MHD equations becomes stiff in this regime. The MHD approximation takes into account not only the gas pressure but also its inertia, which may become important both far away from the star, in the wind zone, and near the light cylinder. Ideally we should also incorporate a physical model for electrical resistivity, which would allow us to conduct a proper study of the dissipation within the equatorial current sheet, but it makes perfect sense to start with the simpler framework of ideal MHD.

4.1 Equations

The system of ideal relativistic MHD includes: the continuity equation

$$\partial_t(\alpha\sqrt{\gamma}\,\rho u^t) + \partial_i(\alpha\sqrt{\gamma}\,\rho u^i) = 0, \tag{24}$$

Figure 1. Representative force-free solution. The contours show the magnetic flux surfaces and the colour image shows H_ϕ. Notice that the magnetic field lines are closed even beyond the light cylinder, $\varpi_{\text{lc}} = 1$.

such field lines cannot have an azimuthal component in the equatorial plane because of the symmetries of the problem. Thus, one may expect spinning up of the charged particles till their inertia becomes important and the centrifugal force opens up the closed field lines.

On the other hand, the drift approximation itself may break down and the charges may start moving across the magnetic field well before their inertia becomes dynamically significant. One can look at this breakdown of the drift approximation from another perspective. Beyond the light cylinder the electric field of a force-free solution becomes stronger than the poloidal component of the magnetic field and thus stronger than the total magnetic field in regions where the azimuthal component of the magnetic field vanishes. Such a strong electric field is capable of 'tearing' charged particle off the magnetic field lines and driving strong electric current across the magnetic field. This is a micro-physical argument but there is an equally compelling macroscopic one. Full opening of magnetic field lines implies an infinitely thin equatorial current sheet with an infinitely high electric current density. Even very small but finite resistivity will destroy this ideal configuration and result in a steady-state current layer of finite thickness and closure of some of the magnetic field lines in this layer. Thus, the only meaningful question is how many field lines will be closed in this layer.

In order to explain the remarkable indifference of our solutions to the value of $\sigma_\perp$, it is instructive to consider a much simpler problem of a one-dimensional current sheet. Here we adopt an inertial frame with Cartesian coordinates so that $\boldsymbol{D} = \boldsymbol{E}$ and $\boldsymbol{H} = \boldsymbol{B}$. Assuming that $\boldsymbol{B} = (0, B^y, 0)$ and $\boldsymbol{E} = (0, 0, E^z)$, and using the following model for the cross-field conductivity,

$$\sigma_\perp = \begin{cases} \sigma_0 & \text{if} \quad E^2 > B^2, \\ 0 & \text{if} \quad E^2 \leqslant B^2, \end{cases} \tag{23}$$

where ρ is the rest-mass density of matter and u^ν is its four velocity; the energy–momentum equations

$$\partial_t \left(\alpha \sqrt{\gamma}\, T^t{}_\nu \right) + \partial_i \left(\alpha \sqrt{\gamma}\, T^i{}_\nu \right) = \tfrac{1}{2} \partial_\nu (g_{\alpha\beta}) T^{\alpha\beta} \alpha \sqrt{\gamma}, \tag{25}$$

where $T^{\nu\mu}$ is the total stress–energy–momentum tensor; the induction equation

$$(1/c)\, \partial_t(B^i) + e^{ijk}\, \partial_j(E_k) = 0; \tag{26}$$

and the divergence-free condition

$$\partial_i(\sqrt{\gamma}\, B^i) = 0. \tag{27}$$

The total stress–energy–momentum tensor, $T^{\mu\nu}$, is the sum of the stress–energy–momentum tensor of matter,

$$T_{(\mathrm{m})}^{\mu\nu} = w u^\mu u^\nu - p g^{\mu\nu}, \tag{28}$$

where p is the thermodynamic pressure and w is the enthalpy per unit volume, and the stress–energy–momentum tensor of the electromagnetic field,

$$T_{(\mathrm{e})}^{\mu\nu} = \frac{1}{4\pi} \left[F^{\mu\gamma} F^\nu{}_\gamma - \tfrac{1}{4} \left(F^{\alpha\beta} F_{\alpha\beta} \right) g^{\mu\nu} \right], \tag{29}$$

where $F^{\nu\mu}$ is the Maxwell tensor of the electromagnetic field. In the limit of ideal MHD,

$$E_i = e_{ijk} v^j B^k / c, \tag{30}$$

where $v^i = u^i/u^t$ is the usual three velocity of plasma.

4.2 Numerical method

The MHD simulations were carried out using a Godunov-type scheme that is described in Komissarov (1999, 2004b). However, we had to introduce some additional features in order to overcome a number of challenging problems specific to the case of highly magnetized plasma.

The MHD equations become stiff in magnetically dominated domains, and this is exactly the case for the main volume of pulsar magnetospheres where the energy density of matter is many orders of magnitude less than that of the electromagnetic field. There is no hope of reaching such conditions with our numerical method. However, the electromagnetic part of the MHD solution should not be very different even when the energy ratio is artificially increased up to 0.1–0.01; errors of the order of a few per cent are quite acceptable at this stage of the investigation. In fact, the results of force-free and MHD simulations of the monopolar magnetospheres of black holes strongly support this conclusion (Komissarov 2001, 2004b). In those MHD simulations, additional plasma was pumped in the regions where its energy density had reached a certain lower limit. Here, we apply a similar trick. The actual condition is

$$w W^2 \geqslant a_{(1)} B^2, \tag{31}$$

where W is the Lorentz factor of plasma and $a_{(1)}$ is a small constant; we used $a_{(1)} = 0.01$. When this condition is broken, we increase both ρ and p in the same proportion so that $w W^2 = a_{(1)} B^2$.

However, dipolar magnetospheres are more challenging compared to monopolar ones because of the faster decline of magnetic field strength with distance from the star and the existence of dead zones. Within the dead zones the magnetospheric plasma is supposed to be in static equilibrium. Thus, the component of the centrifugal force acting along the magnetic field lines has to be balanced by some other force. It has been argued that the dead zone plasma is charge-separated and the force balance is achieved by means of a small parallel component of the electric field (e.g. Holloway & Price

1981; Mestel 1999). However, the recent eclipse observations of the binary pulsar JO737−3039 allowed direct measurement of the particle density in the dead zone of one of the components (Lyutikov & Thompson 2005). It has turned out to be many orders of magnitude higher than the expected density of the charge-separated plasma. Whether such a high density is specific for binary systems only, as proposed in Lyutikov & Thompson (2005), or typical for single pulsars as well remains to be seen. In any case, the charge-separated dead zones cannot be modelled within the MHD approximation where the required force balance can only be achieved by means of gas pressure. This would require the gas pressure to increase along the magnetic field line and reach a maximum in the equatorial plane. On the contrary, the magnetic pressure of a dipolar magnetosphere decreases with distance as r^{-6} and thus the ratio of magnetic to gas pressure has to decline even faster than r^{-6}. Given the requirement on the dead zone to remain magnetically dominated everywhere, this implies very high pressure ratio near the star surface – much higher than our numerical scheme can accommodate. To overcome this problem one could consider the case where the star radius is only 2–3 times smaller than the radius of its light cylinder, but this would have a rather strong effect on the structure of the magnetosphere. This is why we have preferred a different strategy.

Its idea is to reduce, somewhat arbitrarily, the dynamical effect of the centrifugal force on the motion of plasma near the star so that it does not destroy the nearly force-free equilibrium across the magnetic field lines within the dead zone. One way of achieving this is to reset the gas pressure and its rest-mass density to some rather low 'target' values, p_s and ρ_s, within the dead zone every time-step. At the same time one may reset the flow speed along the magnetic field lines to zero, just as it should be in equilibrium. However, the dead zone is not a well-defined region in the case of time-dependent magnetospheres. Instead, one could apply the same procedure to a volume that is guaranteed to include, if not the whole dead zone, then at least its inner part. For example, we used a sphere of radius $r_s \leqslant \varpi_{\mathrm{lc}}$. However, this leads to another complication – in the open field region bounded by the sphere there emerges a strong rarefaction wave, so strong that the code crashes. Fortunately, this can be avoided if, instead of resetting the target values, one introduces a relaxation towards them with the relaxation time gradually increasing towards the boundary of the relaxation domain. We evolved p, ρ and $v_\parallel$ according to the following equations:

$$\frac{\mathrm{d} v_\parallel}{\mathrm{d} t} = -b_{(1)} v_\parallel, \tag{32}$$

$$\frac{\mathrm{d} p}{\mathrm{d} t} = -b_{(2)}(p - p_s), \tag{33}$$

$$\frac{\mathrm{d} \rho}{\mathrm{d} t} = -b_{(2)}(\rho - \rho_s), \tag{34}$$

where

$$b_{(1)}(r) = b_{(0)} f(r), \tag{35}$$

$$b_{(2)}(r, \theta) = b_{(1)} |\cos\theta|, \tag{36}$$

$$f(r) = \begin{cases} (r_s - r)/(r_s - r_*) & \text{if} \quad r < r_s, \\ 0 & \text{if} \quad r > r_s, \end{cases} \tag{37}$$

where $b_{(0)}$ is constant and r_* is the star radius. As one can see, the relaxation time becomes infinite at $r = r_s$. The results presented below correspond to $r_s = \varpi_{\mathrm{lc}}$. However, we have also tried smaller values of r_s in order to verify that this does not lead to qualitatively

different results. (We discuss the effects of reducing r_s in Section 5.) The dependence of $b_{(1)}$ on the azimuthal angle was introduced in order to reduce the possible adverse effect on the current sheet should it be formed inside the light cylinder. The actual value of $b_{(0)}$ is to be found by the method of trial and error. Finally, we use the following targets for the pressure and density:

$$p_s = a_{(2)}\rho_s c^2, \qquad \rho_s c^2 = a_{(1)} B^2, \qquad (38)$$

where $a_{(1)} = 0.01$ and $a_{(2)} = 0.001$.

In these simulations, the computational grid covered the axisymmetric domain $(r, \theta) = [0.1, 50] \times [0, \pi]$, and hence the star radius was set to $r_* = 0.1$. In order to speed up the calculation we started with a relatively low-resolution grid, 124×61, and then increased the resolution twice after the solution seemed to have reached a steady state on the scale of several ϖ_{lc}. Hence the final grid had 496×244 cells.

4.3 Results

The initial solution described a non-rotating magnetosphere with dipolar magnetic field (equation 3), $v^i = 0$, $\rho = \rho_s$ and $p = p_s$. At $t = 0$ the star rotation is switched on and a torsional Alfvén wave is emitted from its surface. As it propagates away, a larger and larger portion of the magnetosphere is set into rotation and develops an electric current system. This process is illustrated in Fig. 2, where the contours show the magnetic field lines and the colour image shows the distribution of $H_\phi = 2(I + I_d)/c$, where I is the total electric current and I_d is the total displacement current through the circular contour of cylindrical radius $\varpi = r \sin \theta$. Unity corresponds to $H_\phi = \mu \Omega^2 c^{-2}$.

Behind the wave the solution gradually approaches a steady state. Fig. 3 shows the inner region of this steady-state solution at $t = 55$, the termination time of the simulations. The structure of the magnetic field lines suggests that the dead zone extends all the way up to the light cylinder. Beyond the light cylinder the poloidal magnetic

field becomes radial, as expected (Ingraham 1973; Michel 1974). Some magnetic field lines are closing up beyond the light cylinder but they do so within the equatorial current sheet due to the finite artificial resistivity in the numerical scheme – it is easy to see the transition between the dead zone and the current sheet within which the magnetic field lines are highly stretched in the radial direction. The colour image in the top left panel of this figure shows the distribution of H_ϕ. Since in a steady state the displacement current vanishes, we have $H_\phi = 2I/c = \mathcal{A}$. This image confirms our conclusion on the extension of the dead zone, which is seen in the image as a toroidal structure with $H_\phi = 0$. (Indeed, within the dead zone the poloidal currents do not flow and H_ϕ must be zero.) The jumps in H_ϕ occurring at the boundary of the dead zone and along the equator are indicators of thin sheets of return current. This image also shows, though not as clearly, that H_ϕ and hence I reach maximum amplitude at some finite distance from the equatorial plane. This indicates the presence of an additional layer of return current that surrounds the equatorial current sheet and the dead zone (Contopoulos et al. 1999).

The current sheets are most prominent in the right panel of Fig. 3, which shows the distribution the poloidal current density, J_p, multiplied by r^2. One can also see that the thickness of the current sheets near the Y-point is about $(0.5–0.6)\varpi_{lc}$ and that the equatorial current sheet extends inside the light cylinder by approximately the same distance.

From time to time it has been suggested that particle inertia may actually become dynamically important near the light cylinder, thus rendering the force-free approximation as unsuitable. The argument develops like this. Provided the magnetospheric plasma simply corotates with the star, its speed would exceed the speed of light beyond the light cylinder. This does not occur because of the rapidly increasing inertial mass of this plasma near the light cylinder. This leads to a very strong centrifugal force that causes the plasma to flow across the light cylinder, thus opening up the magnetic field lines and sweeping them back. However, this is not what occurs in
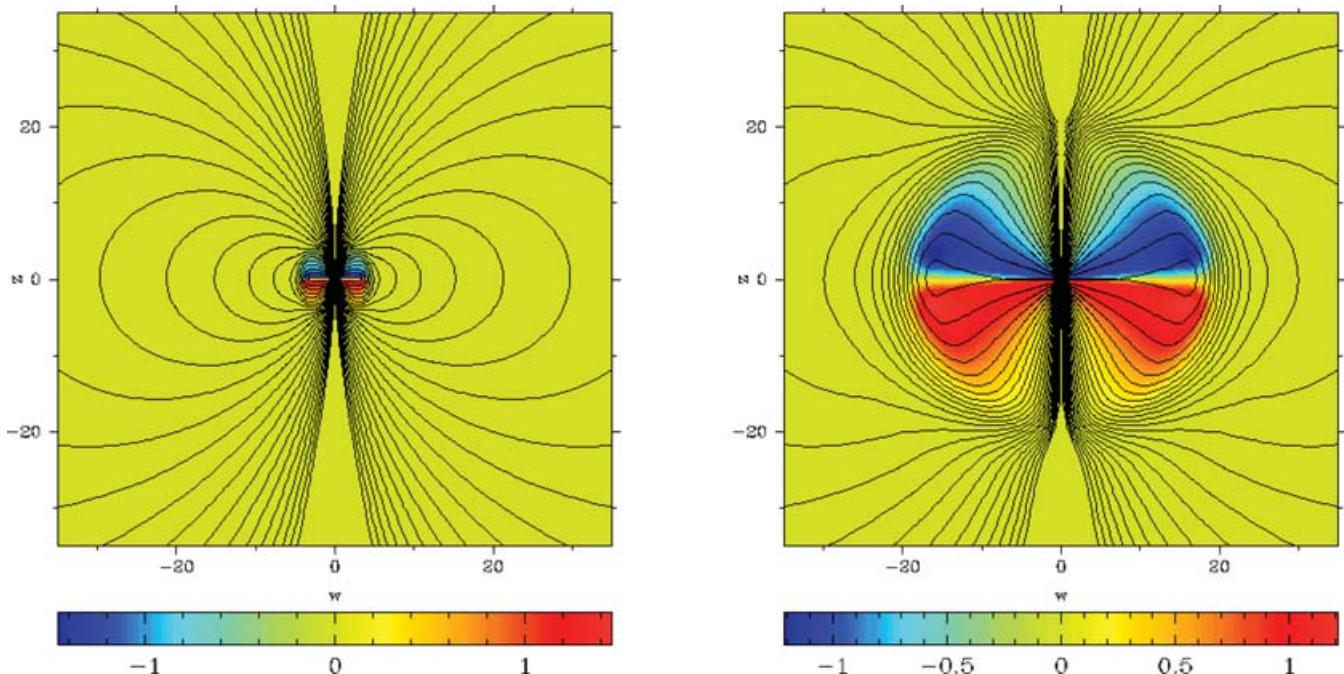
Figure 2. The evolution of a spun-up dipole. This figure shows the solution at $t = 5$ (left) and at $t = 20$ (right). The contours show the magnetic flux function, $\log_{10} \Psi$, and the colour image shows $H_\phi = 2(I + I_d)/c$, where I is the electric current and I_d is the displacement current.
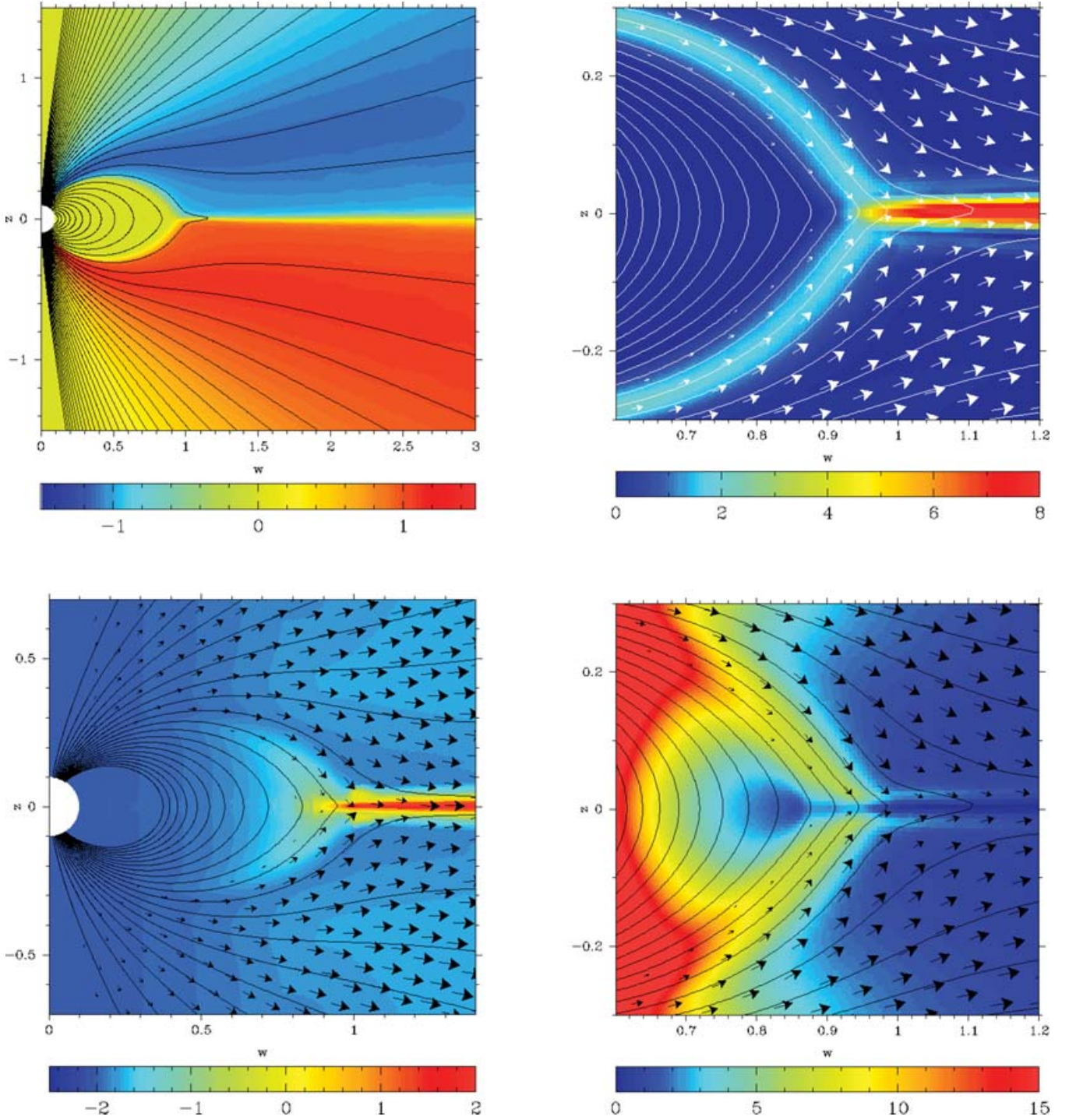
Figure 3. Inner part of the solution at $t = 55$. Top left: The contours show the magnetic flux function, Ψ, and the colour image shows H_ϕ. Top right: The contours show the magnetic flux function, Ψ, the arrows show the flow velocity, and the colour image shows the magnitude of the poloidal electric current density multiplied by r^2. Bottom left: The contours show the magnetic flux function, the arrows show the flow velocity, and the colour image shows $\log_{10}(wW^2/B^2)$. Bottom right: The contours show the magnetic flux function, the arrows show the flow velocity, and the colour image shows B^2.

our simulations. Indeed, the top left panel of Fig. 3 shows that, very much in agreement with the force-free models, H_ϕ is constant along the magnetic flux surfaces even when they cross the light cylinder. Moreover, this conclusion is fully supported by the data presented in the bottom left panel of Fig. 3, which shows the distribution of wW^2/B^2, the quantity that can be used to describe the relative im-

portance of the inertial effects as well as of the gas pressure. One can see that it remains very low everywhere outside of the equatorial current sheet, including the light cylinder.

There is, however, one location in the force-free solution of Contopoulos et al. (1999) where the inertial effects are expected to become important. It is the so-called Y-point, i.e. the point where

the dead zone approaches the light cylinder. Indeed, since the dead zone corotates with the star, then plasma particles attached to its field lines rotate with a speed reaching the speed of light at the Y-point. Moreover, one may argue that the divergence of the magnetic field strength at the Y-point discovered by Gruzinov (2005) also suggests a breakdown of the force-free approximation. This fully agrees with the data presented in the bottom right panel of Fig. 3, which shows the distribution of B^2 in our MHD solution. Although the plot shows a local minimum at $(z, \varpi) = (0, 0.85)$ and then some growth of B^2 in the direction of the Y-point, this growth never develops. Moreover, in our solution the poloidal magnetic field lines approach the Y-point at an angle of $\simeq 50$ degrees to the equatorial plane (see Fig. 3), which is significantly lower than 77.3 degrees predicted by Gruzinov (2005) and quite close to the value of 56.5 degrees found in Goodwin et al. (2004). In addition to the inertial effects, the relatively high thickness of the current sheets near the Y-point (the right top panel of Fig. 3) and finite gas pressure also contribute to these discrepancies between our simulations and the force-free solution. Our results, however, do not prove that the asymptotic force-free solution for the Y-point is irrelevant. It seems possible that for sufficiently high magnetization and small resistivity the exact MHD solution will first approach the force-free asymptote found by Gruzinov and then deviate from it on smaller scales. This, however, requires further investigation.

Fig. 4 shows H_ϕ as a function of Ψ at $r = 1.1$ and allows us to see these details of the current system more clearly. This distribution is very similar to the one given in fig. 4 of Contopoulos et al. (1999). The minimum has

$$\Psi_{\min} \simeq 1.02 \frac{\mu\Omega}{c} \quad \text{and} \quad A_{\min} \simeq 1.12 \frac{2\mu\Omega^2}{c^2}.$$

The left panel of Fig. 5 shows the distribution of the magnetic flux function Ψ in the equatorial plane of the final solution. As a consequence of the finite artificial resistivity in our numerical scheme, the magnetic field lines continue to close up even beyond the line cylinder, and this shows itself via a systematic decline of Ψ at $r > 1$. Thus, it is not so straightforward to determine the fraction of opened field lines in this solution. One way to describe it quantitatively is by giving the value of the flux function exactly
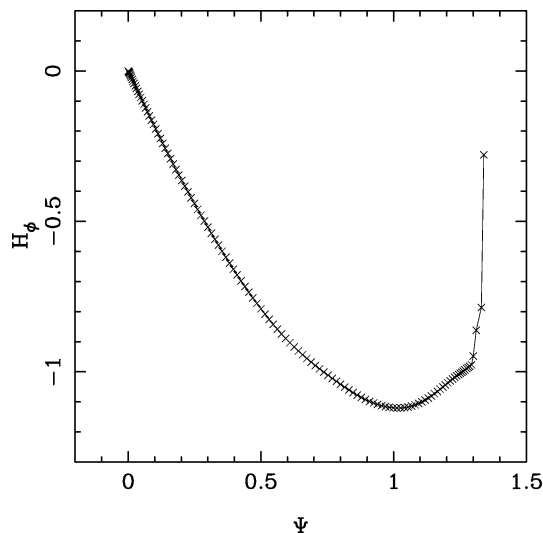
Figure 4. Plot of H_ϕ as a function of the magnetic flux function Ψ on the sphere $r = 1.1$ at time $t = 55$.

at $(\theta = \pi/2, r = 1)$. This gives us

$$\Psi_{\mathrm{yp}} \simeq (1.37\text{–}1.38) \frac{\mu\Omega}{c}. \tag{39}$$

On the other hand, Fig. 5 shows that the decline of Φ significantly slows down at $r > 2$ where Φ reaches the value of

$$\Psi_{\mathrm{open}} \simeq (1.26\text{–}1.27) \frac{\mu\Omega}{c}. \tag{40}$$

These numbers should be compared with the values $c\Psi_{\mathrm{open}}/\mu\Omega = 1.23$ in Contopoulos (2005) and Timokhin (2005), 1.27 in Gruzinov (2005) and 1.36 in Contopoulos et al. (1999).

The right panel of Fig. 5 shows the total flux of energy through a sphere of radius r, which should be constant in a steady-state solution. One can see that it is indeed more or less constant, with the exception of $1 < r < 2$ where the energy flux slightly increases. This increase is a permanent feature that arises because our scheme is not strictly conservative. In order to evaluate the spin-down power of the star, we used the energy flux through a sphere of radius $r = 1$, thus ignoring the non-physical increase of total luminosity beyond $r = 1$. This gives us

$$L \simeq 1.1 \frac{\mu^2\Omega^4}{c^3}, \tag{41}$$

which is in a very good agreement with the result by Gruzinov (2005).

Fig. 6 shows the distribution of the angular velocity of magnetic field lines, Ω_{f}. In the exact steady-state force-free solution the magnetic field lines rotate with same angular velocity as the star,

$$\Omega_{\mathrm{f}} = \Omega. \tag{42}$$

However, in our solution, Ω_{f} noticeably deviates from Ω inside the layer coincident with the current sheet between the open field lines and the dead zone (see Fig. 6). The most likely reason for this is the enhanced numerical resistivity in the current sheet. The comparison of solutions with different numerical resolution (Fig. 6) shows that the thickness of the layer significantly decreases with resolution. However, the amplitude of the perturbations does not seem to depend on the resolution.

Fig. 7 shows that, far away from the star, the distribution of poloidal field lines is very similar to the split-monopole one. This is exactly what was concluded in the pioneering papers by Ingraham (1973) and Michel (1974) on the force-free magnetospheres. More recently, the centrifugally driven outflows in split-monopole magnetospheres have been studied within the cold MHD approximation. According to these studies the Lorentz factor of centrifugally accelerated plasma at the fast critical point is

$$W = \sigma^{1/3}, \tag{43}$$

where σ is the so-called magnetization parameter, which is defined as the ratio of the Poynting flux density to the rest mass–energy flux density at the footpoint of the magnetic field line (Beskin 1997). For outflows that are initially Poynting-dominated, $\sigma \simeq \tilde{\sigma}$, where $\tilde{\sigma}$ is the ratio of the total energy flux density to the rest mass–energy flux density. In contrast to σ, $\tilde{\sigma}$ can be measured at every point of the field line, as it is constant along it. Fig. 8 shows the distributions of $\tilde{\sigma}$, W and the ingoing speed of the fast wave in the radial direction along the ray $\theta = 1$ rad. From these data we find that along this ray $\sigma \simeq 77$ and the fast point is located at $r \simeq 6.8$ where $W \simeq 4.3$. On the other hand, we can use the above value of σ in order to calculate the Lorentz factor at the fast point directly from equation (43) – this gives us $W = 4.25$. Thus, the split-monopole model provides quite a good model for the wind zone of an aligned magnetic dipole.
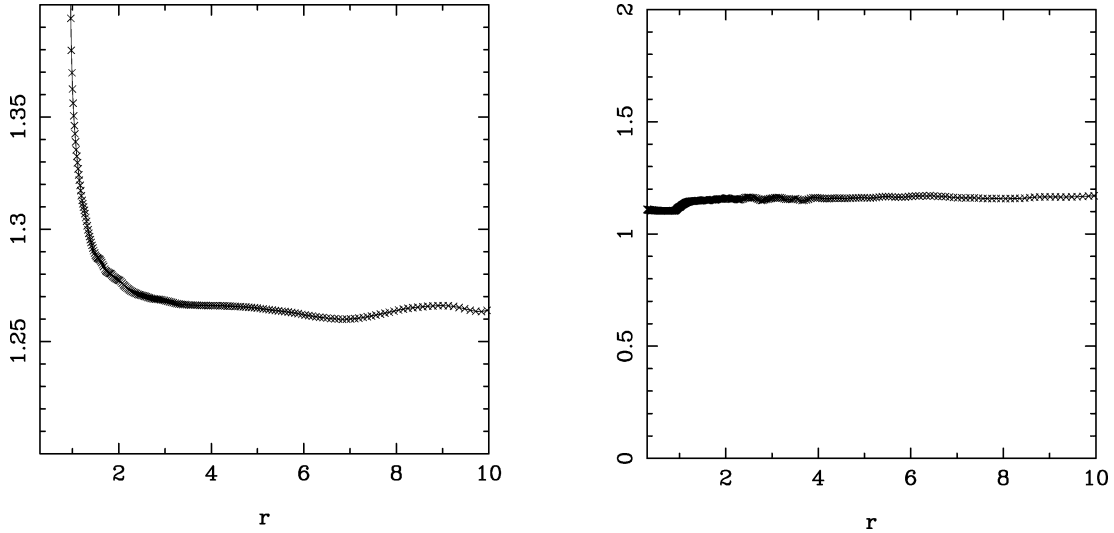
Figure 5. Left: The magnetic flux function, Ψ, in the equatorial plane as a function of r at time $t = 55$. Right: The total energy flux through a sphere of radius r at time $t = 55$.
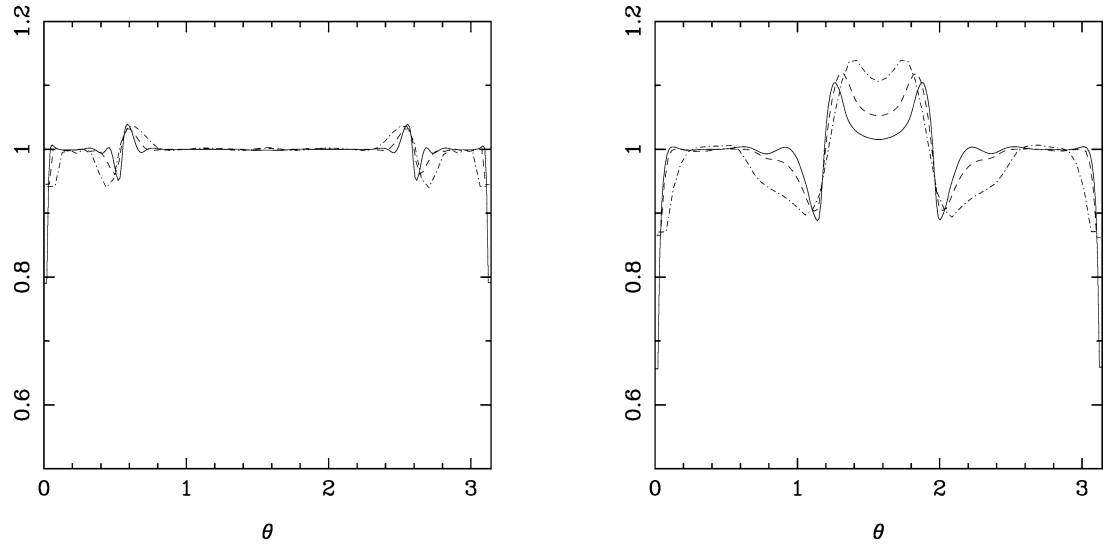
Figure 6. The angular velocity distribution at $t = 55$ within the light cylinder at $r = 0.2$ (left) and at $r = 0.7$ (right). The dot-dashed, dashed and solid lines show the solutions with 61, 122 and 244 cells in the θ-direction.

Another interesting feature of Fig. 7 is the significantly higher value of the Lorentz factor of the outflow within the equatorial current sheet. This suggests that the mechanism of the flow acceleration is somewhat different there. The obvious suspect is heating due to resistive dissipation of the electromagnetic energy. The high value of the Lorentz factor in the current sheet suggests that its contribution to the global energy transfer can be quite significant.

The left panel of Fig. 9 shows the evolution of the wind luminosities with distance from the star by the end of the simulations. The total luminosity is more or less constant apart from noticeable perturbations around $r = 17$, 30 and 45. The big bump around $r = 45$ is related to the leading front of the wind. The perturbations around $r = 17$ and 30 are related to the grid refinement events – each time the computational grid is refined the numerical solution evolves to a slightly different state, most of all in the inner region of the computational domain. This triggers noticeable waves propagating away from the star. The electromagnetic luminosity, which is shown in

Fig. 9 by the dashed line, gradually decreases with distance, thus indicating the ongoing conversion of electromagnetic energy into hydrodynamic energy. This is supported by the evolution of the hydrodynamic luminosity of the wind, which is shown by the dash-dotted line. One of the interesting features of this line is its rapid initial rise, which suggests particularly effective energy conversion. The nature of this conversion is clarified in the right panel of Fig. 9, which shows that the current sheet accounts for about 70 per cent of the total hydrodynamic luminosity at $r = 10$ and this corresponds to about 15 per cent of the total wind luminosity. This clearly points to Ohmic heating in the current sheet as being the main source of energy conversion.

5 DISCUSSION

There is not much to discuss in connection with our force-free simulations of pulsar magnetospheres. We simply have not been able
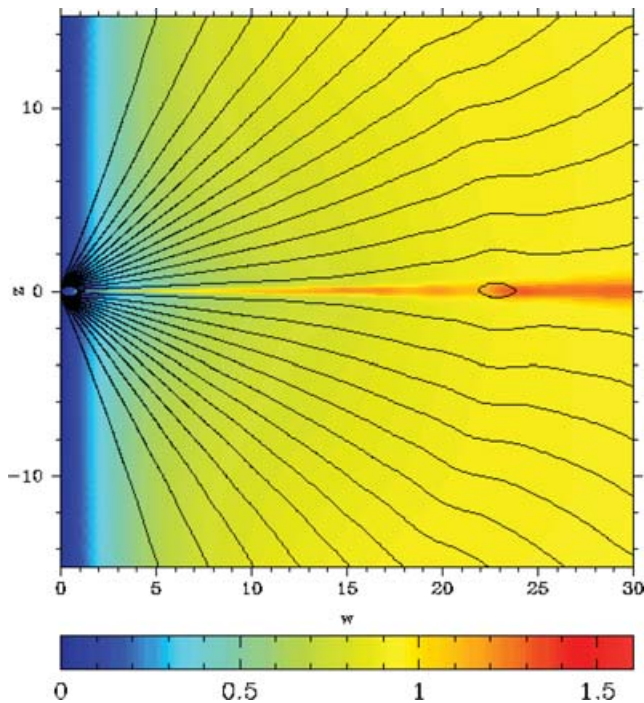
Figure 7. The wind zone structure of a dipolar magnetosphere. The contours show the field lines of poloidal magnetic field. The colour image shows the distribution of $\log_{10} W$.

to make the required progress using this framework because of the inability to handle the equatorial current sheet. For this reason we will focus in this section almost entirely on the results of our MHD simulations and their possible implication for pulsar physics.

One of the key goals of this study was to determine whether the MHD equations allow stable, or quasi-stable, steady-state solutions for dipolar axisymmetric magnetospheres of neutron stars. This problem has become particularly interesting since the discovery of a whole family of steady-state force-free solutions continuously parametrized by the location of their Y-point (Goodwin et al. 2004; Timokhin 2005). Our results indicate the existence of a unique steady-state MHD solution to the problem, and this solution is very close to the force-free stationary solution of the pulsar equation with Y-point located at the light cylinder – the original solution of the pulsar equation found by Contopoulos et al. (1999). Why this solution is preferable to those whose Y-point is located well inside the light

cylinder has already been explained in Contopoulos (2005). If the resistivity is not vanishingly small, then, even if the initial solution had the dead zone buried well inside the light cylinder, it would take only a finite time for the antiparallel field lines of the current sheet between the Y-point and the light cylinder to reconnect and form closed loops that become part of the dead zone. The reconnection should also occur beyond the light cylinder, but there the outflow is super-Alfvénic, so the net outcome of the reconnection is likely to be the development of magnetic islands carried by the wind away from the star (Uzdensky 2004). The rate of reconnection depends on the actual resistivity in the current sheet, and in our simulations the resistivity is purely artificial. However, the ultimate outcome is unlikely to be different. Indeed, since the particle inertia on the closed field lines located well inside the light cylinder of pulsar magnetospheres is extremely small, there is no restoring force that would make these field lines open up again. This is supported by the fact that the total electromagnetic energy of the force-free magnetosphere is minimum when the Y-point is located on the light cylinder (Timokhin 2005).

At this point it makes sense to discuss whether the relaxation procedure applied within $r_s = \varpi_{lc}$ (see Section 4.2) could somehow promote the expansion of the dead zone towards the light cylinder. As we have already pointed out in Section 4.2, all relaxation times gradually increase towards infinity as $r \to r_s$. Thus, near the light cylinder the effect of the relaxation procedure on the flow is increasingly small. Moreover, the relaxation time for the gas pressure becomes infinite at $\theta = \pi/2$. This would allow the buildup of gas pressure required to support the equatorial current sheet should it exist within the light cylinder. However, in order to resolve this issue fully, we carried out additional simulations with the radius of the relaxation sphere pushed down to $r_s = 0.7\varpi_{lc}$. Fig. 10 allows comparison of the two solutions with regard to the location of the Y-point. The colour image in this figure shows the distribution of H_ϕ; the solid lines show the magnetic surfaces for the model with $r_s = 0.7\varpi_{lc}$; whereas the dashed lines show the magnetic surfaces for the model with $r_s = \varpi_{lc}$. As one can see, more field lines open up for smaller r_s, and this is caused by the increased dynamical role of the centrifugal force. However, the location of the Y-point remains basically the same. Thus, our relaxation procedure cannot be considered as the reason for the dead zone extending all the way up to the light cylinder.

Contopoulos (2005) also pointed out that the open field lines of pulsar magnetospheres may rotate at a slower rate than the closed field lines of the dead zone as a result of the finite potential gap of the polar cap. In particular, he speculated about the possibility of
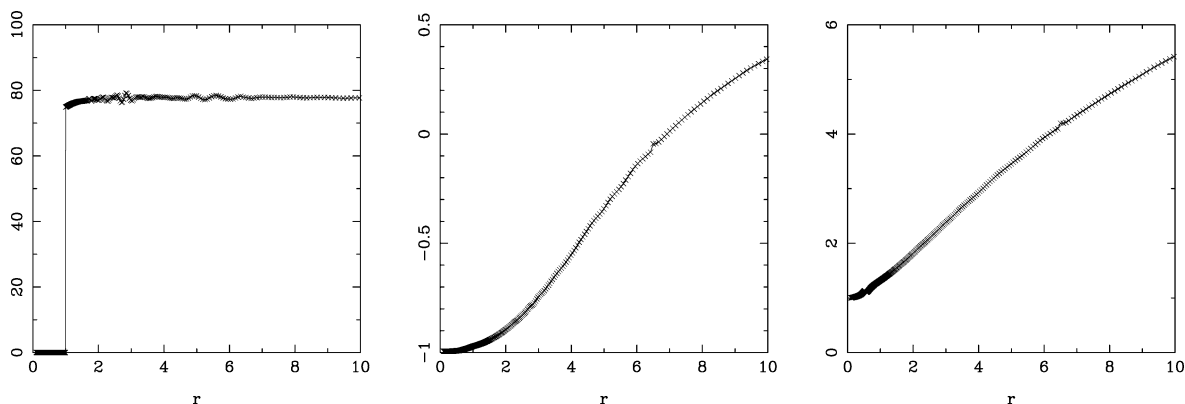
Figure 8. The variation of a number of key parameters along the ray $\theta = 1$. Left: The local magnetization parameter $\tilde{\sigma}$. Middle: The wave speed of the ingoing fast wave in the radial direction (the speed of light $c = 1$). Right: The Lorentz factor of the wind.
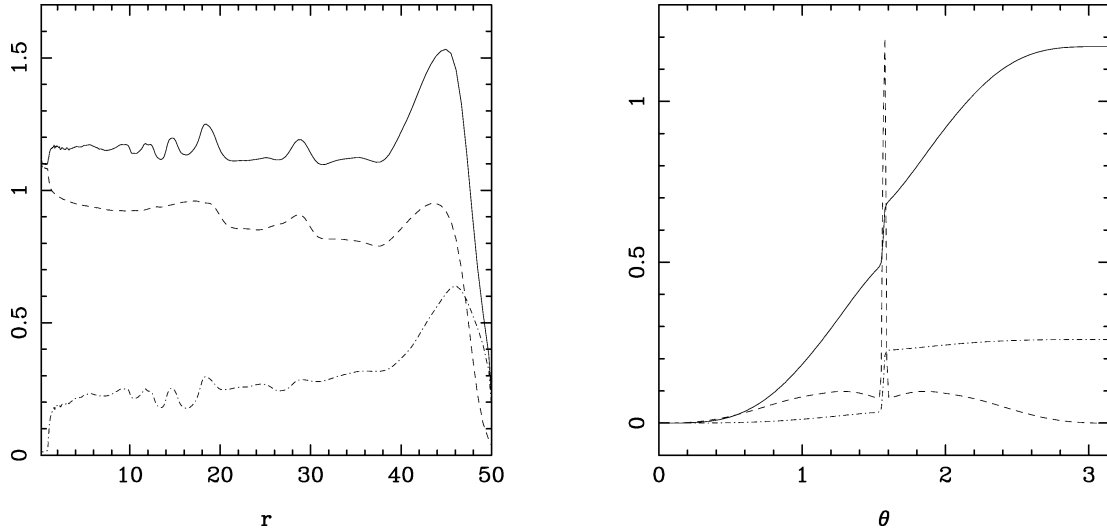
Figure 9. Conversion of the electromagnetic luminosity into the hydrodynamic luminosity of the wind. Left: The total luminosity (solid line), the electromagnetic luminosity (dashed line), and the hydrodynamic luminosity (dot-dashed line) of the wind at $t = 55$. Right: The angular distribution of the total luminosity at $r = 10$. The solid line and the dot-dashed line show the total luminosity and the hydrodynamic luminosity within the polar cone of angle θ respectively; the dashed line shows the total flux density in the radial direction.
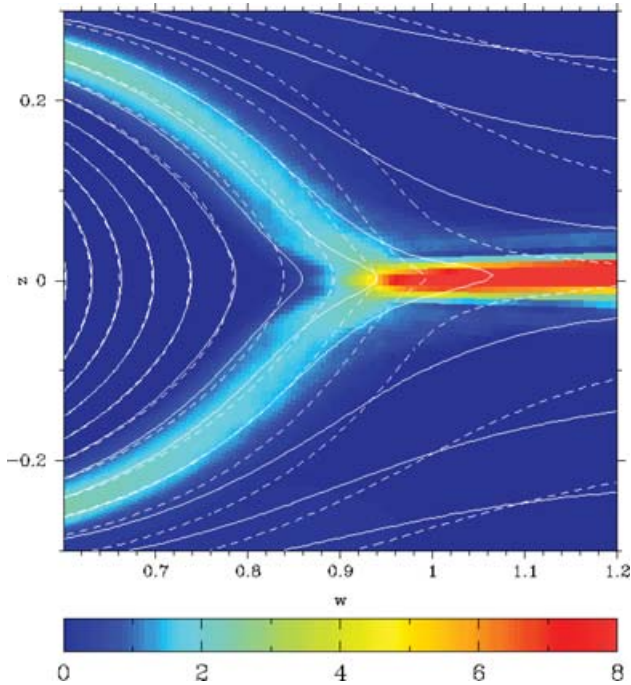
Figure 10. Comparison of solutions with relaxation domains of different sizes. The colour image shows H_ϕ and the solid lines show the magnetic flux function for the model with $r_s = 0.7\varpi_{lc}$. The dashed lines show the magnetic flux function for the model with $r_s = \varpi_{lc}$.

a significant growth of the polar gap due to a sudden decrease of the particle injection rate in the gap in order to explain explosive phenomena like the 2004 December 27 burst in SGR 1806−20. Although it is not clear what could cause such a sudden incident of 'charge starvation', it was suggested long ago that a slow systematic evolution of the polar gap could result from the gradual spin-down of the star (Sturrock 1971; Ruderman & Sutherland 1975). Thus, differentially rotating magnetospheres are not just interesting theoretical models but can have great relevance for real pulsars.

Contopoulos (2005) found force-free stationary numerical solutions for such magnetospheres in the simple case of a uniformly rotating polar cap and a uniformly rotating dead zone, which was assumed to corotate with the star. [In fact, the dead zone may also have a potential gap that separates electric charges of opposite sign, but it is expected to be rather small (Holloway & Price 1981).] These solutions have two light cylinders – a smaller one for the dead zone and a larger one for the open field lines – and the dead zone extends all the way up to its light cylinder. Contopoulos (2005) argued that, although there existed solutions with a smaller dead zone, they were not sustainable due to reconnection in the part of the equatorial current sheet that runs between the Y-point and the light cylinder of the dead zone.

In fact, the numerical models constructed by Contopoulos (2005) are likely to be globally unstable to reconnection too. Indeed, in these models the equatorial current sheet continues inside the light cylinder of an open magnetosphere and magnetic reconnection occurring in this region should lead to creation of new closed field lines. However, this case is somewhat more involved. Let us imagine that such reconnection has indeed occurred. The field lines that have just closed down are now beginning to spin-up and corotate with the dead zone. However, they extend beyond the light cylinder of the dead zone and for this reason they cannot corotate with it – as they spin up they begin opening up again. Once they have been opened up, they begin to slow down, thus creating conditions for the next closing down event, and so on. This simple analysis suggests that such differentially rotating magnetospheres cannot be stationary and have to develop oscillations. The typical time-scale of such magnetospheric oscillations seems to be determined by the spin-up time, which must be comparable with the time required for an Alfvén wave to cross the distance between the light cylinder of the dead zone and the star back and forward. Since the Alfvén speed is relativistic and the magnetic field has a significant radial component, the crossing time has to be comparable with the rotational period of the star. The reconnection rate is more likely to affect the amplitude of these oscillations rather than their time-scale, a quicker reconnection leading to a larger fraction of magnetic field lines involved in this process of closing down and opening up. We want

to speculate that these oscillations may be relevant to the origin of the subpulses of radio pulsars (e.g. Manchester & Taylor 1977). For periodic magnetospheric oscillations we would have a phenomenon reminiscent of beating waves – this may explain the so-called drifting subpulses. However, one may also expect quasi-periodic and even chaotic oscillations, and they would result in a much more complicated behaviour of subpulses.

Our MHD solution has a number of interesting features that could not possibly be found in the ideal force-free solution of Contopoulos et al. (1999). Some of them do not depend much on the details of resistivity, like, for example, the centrifugal acceleration of the wind outside of the current sheet. Others, like the Ohmic dissipation and the wind acceleration in the equatorial current sheet, do, and we have to exercise a reasonable degree of caution when interpreting them – MHD simulations with only artificial resistivity can provide at most a qualitatively correct description of such features. However, it is interesting that the dissipation of electromagnetic energy in the equatorial current sheet has already been considered as a promising explanation of the high-luminosity γ-ray emission from young pulsars (Lyubarskii 1996; Kirk, Skjæraasen & Gallant 2002). Given the fact that these γ-rays carry away a significant fraction of the spin-down power, up to 10 per cent in the most extreme examples (Thompson 2001), and that pulsar magnetospheres are highly magnetically dominated, an efficient dissipation of Poynting flux somewhere in the magnetosphere is needed to explain these observations, and the equatorial current sheet is one of the most natural locations for such dissipation. In particular, Lyubarskii (1996) argued that this high-energy emission originates from the current sheet just beyond the dead zone (this is exactly where our simulations show most effective Ohmic dissipation). The polarization observations of the optical emission from the Crab pulsar support this idea. This emission is found to be polarized parallel to the rotation axis at the peaks of the pulses and between the pulses (within the pulses the polarization vector rotates, which may be attributed to the rotation of the magnetosphere). This shows that the magnetic field of the emitting region is predominantly perpendicular to the rotation axis, as it should be if this radiation is generated in the equatorial current sheet.

ACKNOWLEDGMENTS

REFERENCES

Asano E., Uchida T., Matsumoto R., 2005, PASJ, 57, 409
Beskin V. S., 1990, Sov. Astron. Lett., 16(4), 286
Beskin V. S., 1997, Uspekhi Fizicheskikh Nauk, 167, 689
Beskin V. S., Gurevich A. V., Istomin Ya. N., 1993, Physics of the Pulsar Magnetosphere. Cambridge Univ. Press, Cambridge
Contopoulos I., 2005, A & A, 442, 579
Contopoulos I., Kazanas D., Fendt C., 1999, ApJ, 511, 351 (CKF)
Goodwin S. P., Mestel J., Mestel L., Wright A. E., 2004, MNRAS, 349, 213
Gruzinov A., 1999, preprint, astro-ph/9902288
Gruzinov A., 2005, Phys. Rev. Lett., 94, 021101
Hibschman J. A., Arons J., 2001, ApJ, 546, 382
Holloway N. J., Pryce M. H. L., 1981, MNRAS, 194, 95
Ingraham R. L., 1973, ApJ, 186, 625
Kirk J. G., Skjæraasen O., Gallant Y. A., 2002, A&A, 388, L29
Komissarov S. S., 1999, MNRAS, 303, 343
Komissarov S. S., 2001, MNRAS, 326, L41
Komissarov S. S., 2002a, MNRAS, 336, 759
Komissarov S. S., 2002b, in Semikhatov A., Vasiliev M., Zaikin V., eds, Proc. 3rd Int. Sakharov Conf. on Physics, Moscow. World Scientific, Singapore, p. 392 (astro-ph/021114)
Komissarov S. S., 2004a, MNRAS, 350, 427
Komissarov S. S., 2004b, MNRAS, 350, 1431
Komissarov S. S., Lyubarsky Y. E., 2004, MNRAS, 349, 779
Kanbach G., Kellner S., Score F. Z., Straubmeier C., Spruit H. C., 2003, in Iye M., Moorwood A. F. M., eds, Proc. SPIE 4841, Instrument Design and Performance for Optical/Infrared Ground-Based Telescopes. SPIE, Bellingham, WA, p. 82
Lyubarskii Y. E., 1990, Sov. Astron., 16, 16
Lyubarskii Y. E., 1996, A&A, 311, 72
Lyutikov M., 2003, MNRAS, 346, 540
Lyutikov M., Thompson C., 2005, ApJ, 634, 1223
Manchester R. N., Taylor J. H., 1977, Pulsars. W. H. Freeman, San Francisco
Mestel L., 1999, Stellar Magnetism. Clarendon Press, Oxford
Michel F. C., 1973, ApJ, 180, L133
Michel F. C., 1974, ApJ, 187, 585
Michel F. C., 1982, Rev. Mod. Phys., 54, 1
Muslimov A. G., Tsygan A. I., 1990, Sov. Astron., 34, 133
Petri J., Kirk J., 2005, ApJ, 627, L37
Punsly B., 2003, ApJ, 583, 842
Ruderman M. A., Sutherland P. G., 1975, ApJ, 196, 51
Scharlemann E. T., Wagoner R. V., 1973, ApJ, 182, 951
Spitkovsky A., 2004, in Camilo F., Gaensler B. M., eds, Proc. IAU Symp. 218, Young Neutron Stars and Their Environment. Astron. Soc. Pac., San Francicso, p. 357
Sturrock P. A., 1971, ApJ, 164, 529
Thompson D. J., 2001, in Aharonian F. A., Völk H. J., eds, AIP Proc. 558, High Energy Gamma-Ray Astronomy. American Institute of Physics, Melville, NY, p. 103
Timokhin A., 2005, astro-ph/0507054
Uchida T., 1997, Phys. Rev. E, 56(2), 2181
Uzdensky D. A., 2003, ApJ, 598, 446
Uzdensky D. A., 2004, Ap&SS, 292, 573

This paper has been typeset from a TEX/LATEX file prepared by the author.